

AD-A246 893

PL-TR-91-2167

Environmental Research Papers, No.1088

E 200 867

2

AN 11-CM FULL-MATRIX POLARIMETRIC RADAR FOR METEOROLOGICAL RESEARCH

James I. Metcalf

Alexander W. Bishop

Richard C. Chanley, MSgt, USAF

Timothy C. Hiett

Pio J. Petrocchi

26 June 1991

DTIC
ELECTE
JAN 15 1992
S B D

APPROVED FOR PUBLIC RELEASE; DISTRIBUTION UNLIMITED.

92-01235



Original contains color
plates. All DTIC reproduct-
ions will be in black and
white.




PHILLIPS LABORATORY
DIRECTORATE OF GEOPHYSICS
AIR FORCE SYSTEMS COMMAND
HANSCom AIR FORCE BASE, MA 01731

02 1 14 017

"This technical report has been reviewed and is approved for publication"

FOR THE COMMANDER



KENNETH M. GLOVER, Chief
Ground Based Remote Sensing Branch
Atmospheric Sciences Division



ROBERT A. McCLATCHEY, Director
Atmospheric Sciences Division

This report has been reviewed by the ESD Public Affairs Office (PA) and is releasable to the National Technical Information Service (NTIS).

Qualified requestors may obtain additional copies from the Defense Technical Information Center. All others should apply to the National Technical Information Service.

If your address has changed, or if you wish to be removed from the mailing list, or if the addressee is no longer employed by your organization, please notify GP/IMA, Hanscom AFB, MA 01731. This will assist us in maintaining a current mailing list.

REPORT DOCUMENTATION PAGE			Form Approved OMB No. 0704-0188	
Public reporting burden for this collection of information is estimated to average 1 hour per response, including the time for reviewing instructions, searching existing data sources, gathering and maintaining the data needed, and completing and reviewing the collection of information. Send comments regarding this burden estimate or any other aspect of this collection of information, including suggestions for reducing this burden, to Washington Headquarters Services, Directorate for Information Operations and Reports, 1215 Jefferson Davis Highway, Suite 1204, Arlington, VA 22202-4302, and to the Office of Management and Budget, Paperwork Reduction Project (0704-0188), Washington, DC 20503.				
1. AGENCY USE ONLY (Leave blank)		2. REPORT DATE 26 June 1991	3. REPORT TYPE AND DATES COVERED Scientific Interim	
4. TITLE AND SUBTITLE An 11-cm Full-Matrix Polarimetric Radar for Meteorological Research			5. FUNDING NUMBERS PE 61102F PR 2310 TA G8 WU 05	
6. AUTHOR(S) James I. Metcalf Alexander W. Bishop Richard C. Chanley, MSgt, USAF Timothy C. Hiett Pio J. Petrocchi				
7. PERFORMING ORGANIZATION NAME(S) AND ADDRESS(ES) Phillips Laboratory (LYR) Hanscom AFB, MA 01731-5000			8. PERFORMING ORGANIZATION REPORT NUMBER PL-TR-91-2167 ERP, No. 1088	
9. SPONSORING/MONITORING AGENCY NAME(S) AND ADDRESS(ES)			10. SPONSORING/MONITORING AGENCY REPORT NUMBER	
11. SUPPLEMENTARY NOTES				
12a. DISTRIBUTION/AVAILABILITY STATEMENT Approved for public release; Distribution unlimited			12b. DISTRIBUTION CODE	
13. ABSTRACT (Maximum 200 words) The Geophysics Directorate operates a unique 11-cm (S-band) coherent polarimetric radar. The radar can transmit signals of alternating orthogonal polarizations, with either circular or linear basis, and receive signals of polarizations identical and orthogonal to that of the transmitted signal. The received signals, comprising logarithmic power and in-phase and quadrature components of both polarizations, are sampled in 50 selectable gates and recorded for off-line analysis. The radar antenna and the polarimetric data acquisition are controlled by interactive computer programs. Measurements are underway to characterize the performance of the radar, describe microphysical attributes of clouds and precipitation, and identify the effects of changing electric fields on the orientations of hydrometeors. Examples of these measurements are shown. Related facilities are described briefly.				
14. SUBJECT TERMS Radar meteorology Polarimetric radar Polarization diversity Cloud microphysics			15. NUMBER OF PAGES 42	
			16. PRICE CODE	
17. SECURITY CLASSIFICATION OF REPORT Unclassified	18. SECURITY CLASSIFICATION OF THIS PAGE Unclassified	19. SECURITY CLASSIFICATION OF ABSTRACT Unclassified	20. LIMITATION OF ABSTRACT SAR	

Accession For	
NTIS GRA&I	<input checked="checked" type="checkbox"/>
DTIC TAB	<input type="checkbox"/>
Unannounced	<input type="checkbox"/>
Justification	
By	
Distribution/	
Availability Codes	
Dist	Avail and/or Special
A-1	



Contents

1. INTRODUCTION	1
2. THE RADAR	2
2.1. Transmitters	2
2.2. Polarization Control	6
2.3. Antenna	8
2.4. Antenna Control	10
2.5. Receivers	17
3. DATA ACQUISITION, DISPLAY, AND ANALYSIS	19
3.1. Real-time Processing, Archive, and Display	19
3.2. Polarimetric Data Acquisition	19
3.3. Analysis	24
4. MEASUREMENTS	25
5. RELATED FACILITIES	31
6. SUMMARY	33
REFERENCES	35

Illustrations

1. Functional Block Diagram of Radar System	3
2. Engineering Diagram of Radar System	4
3a. Menus of the Antenna Control Program, I	11
3b. Menus of the Antenna Control Program, II	12
3c. Menus of the Antenna Control Program, III	13
3d. Menus of the Antenna Control Program, IV	15
3e. Menus of the Antenna Control Program, V	16
4. Functional Block Diagram of Data Acquisition System	20
5a. Display of Data Acquisition Control Program, I	22
5b. Display of Data Acquisition Control Program, II	23
6. Radar Measurements of Light Rain at Vertical Incidence	27
7a. Radar Observation of Melting Precipitation, I	28
7b. Radar Observation of Melting Precipitation, II	29
8. Radar Observation of Lightning and Changing Electric Fields	32

Table

1. Typical Parameters of Switchable Circulator Network	8
--	---

Preface

This report describes the 11-cm (S-band) Doppler radar operated by the Ground Based Remote Sensing Branch of the Geophysics Directorate (formerly Air Force Geophysics Laboratory) and presents some of the first polarimetric measurements derived from it. This radar is unique at its wavelength not only for combining coherent and dual-channel reception but also for combining pulse-to-pulse switching and dual-channel reception. The ideas that led to the development of this radar were formulated and refined over a period of nearly 15 years. Many people participated in this process. A series of contracts with Georgia Institute of Technology supported the development of theoretical concepts and plans for modifying the radar. At Georgia Institute of Technology, Mr. James Ussailis had a key role in the radar system design study and in the evaluation of high-power microwave switching devices. Mr. Kenneth Glover, Chief of the Ground Based Remote Sensing Branch, monitored some of the contracts; he has strongly supported the program at every stage.

Engineers and technicians in the Ground Based Remote Sensing Branch have been responsible for much of the design, construction, and installation of key components of the radar system. Staff Sgt. Richard D. Curl, Sgt. Anthony DiMascolo, and Sgt. Travis Wood constructed and installed the waveguide and coaxial cables to connect the switchable circulators to the

transmitters, antenna, and receivers under the supervision of Master Sgt. Richard Chanley; all four received the Air Force Achievement Medal for their efforts. Mr. Graham Armstrong designed the real-time data processor and constructed it with the aid of Mr. William Smith. Some of the components were designed by the Design and Analysis Branch and constructed by the Experimental and Structural Support Branch of the Phillips Laboratory. Measurements of several components of the system were performed with valuable assistance from the Ipswich Electromagnetic Measurement Facility of the Rome Laboratory (formerly Rome Air Development Center). Principal responsibilities of the authors of this report, in relation to the polarimetric radar, are the following: Dr. James Metcalf, acquisition and analysis of data; Mr. Alexander Bishop and Master Sgt. Chanley, microwave components and receivers; Mr. Timothy Hiett, data acquisition system; and Mr. Pio Petrocchi, antenna control program.

An 11-cm Full-Matrix Polarimetric Radar for Meteorological Research

1. INTRODUCTION

The 11-cm wavelength (S-band) Doppler radar operated by the Geophysics Directorate in Sudbury, Mass.,¹ has been used for several years for investigations of the physics and kinematics of storms, including both convective storms, typical of the late spring and summer, and synoptic scale low-pressure systems, typical of the fall and winter. Since 1985 this radar has undergone a series of modifications to enable the measurement of polarization-dependent backscatter. Measurements of the linear polarization differential reflectivity (Z_{DR}) were reported previously.^{2, 3} We are now able to measure the full matrix of backscattered signals, based on either linear or circular polarization. The microwave circuitry enables the radar to transmit successive pulses with alternating polarization (either horizontal and vertical or right and left circular) and to receive signals with

(Received for publication 25 June 1991)

(The list of references begins on page 35)

polarizations identical and orthogonal to that of the transmitted signal. A functional block diagram of the system is shown in Figure 1. The first full-matrix measurements were made on 29 January 1990. In these and subsequent observations we have attempted to characterize the polarimetric attributes of the radar as well as to investigate the microphysical aspects of clouds and precipitation. Our primary goal at present is to observe the orientations of hydrometeors affected by electric fields in clouds.⁴

This report describes the polarimetric radar (Section 2) and data acquisition system (Section 3) and presents some of our early measurements (Section 4). Related facilities are described in Section 5. This report thus serves both as a scientific progress report and as a user's guide for the radar. We encourage inquiries by any individuals who are interested in using the radar for scientific investigations.

2. THE RADAR

The radar system comprises two transmitters, polarization control microwave components, dual-port antenna, and receivers. These are described in the following subsections with particular emphasis on polarimetric measurements. Key components of the system are shown in Figure 2.

2.1. Transmitters

The radar was installed originally with two transmitters, operating at wavelengths of 10.87 and 11.07 cm (frequencies of 2.76 and 2.71 GHz), respectively, for the purpose of using different pulse repetition frequencies to resolve ambiguities of range and Doppler velocity. The transmitters, originally built by the Bendix Corp. in the late 1950's for FPS-18 radars, have been highly modified by the Ground Based Remote Sensing Branch, with support from other sections of the laboratory, to increase their reliability, simplify maintenance, and reduce operating costs. Most of the original components that used vacuum tubes have been replaced by solid state components. Input signals for the phase-locked radio-frequency (RF)

Geophysics Directorate Polarimetric Radar

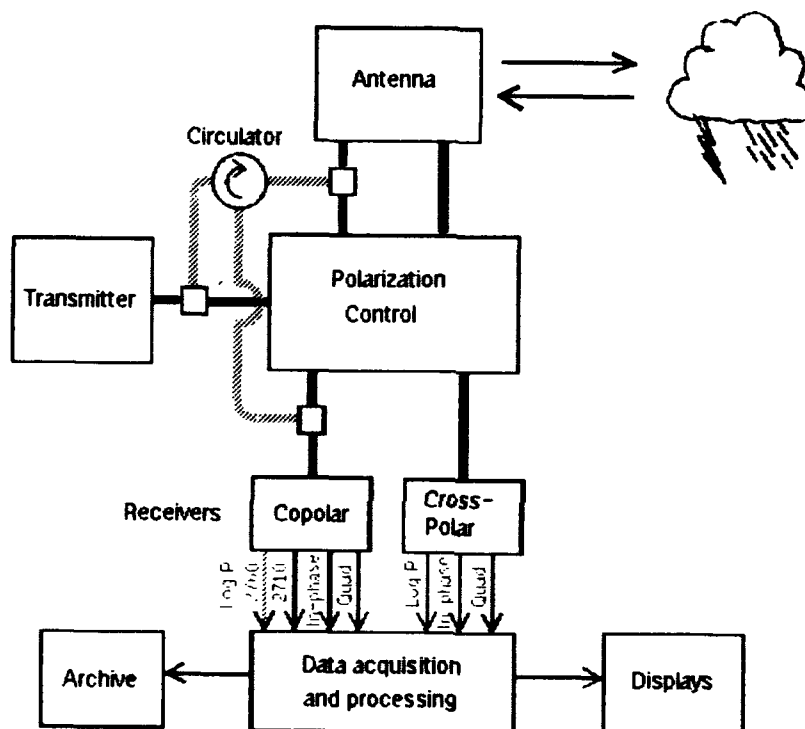


Figure 1. Functional Block Diagram of the Radar System. Key elements discussed in the text include transmitters, polarization control, antenna, receivers, and data acquisition. Elements connected by stippled lines represent the "bypass" used for dual-frequency operation and the resulting additional logarithmic power output.

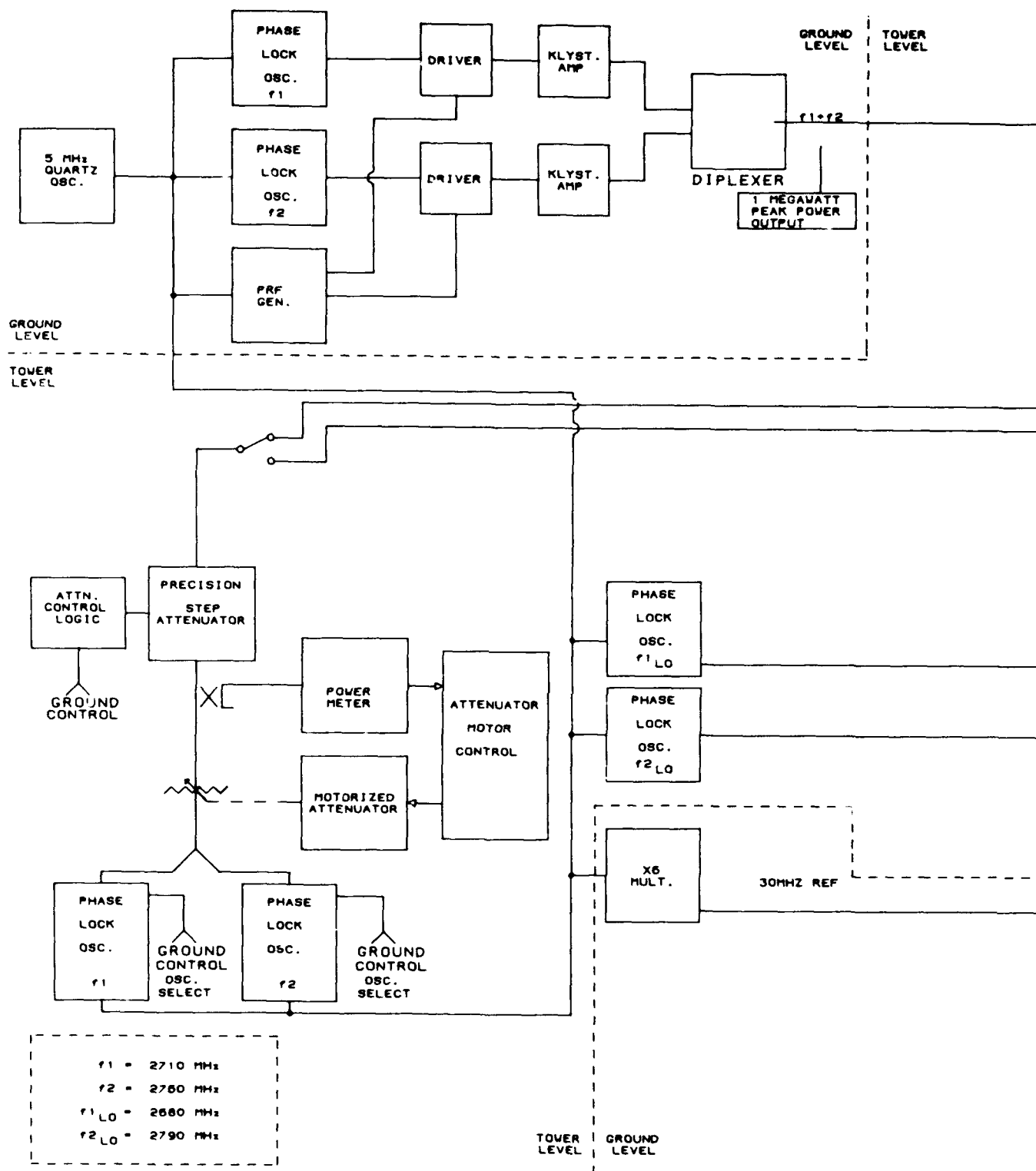
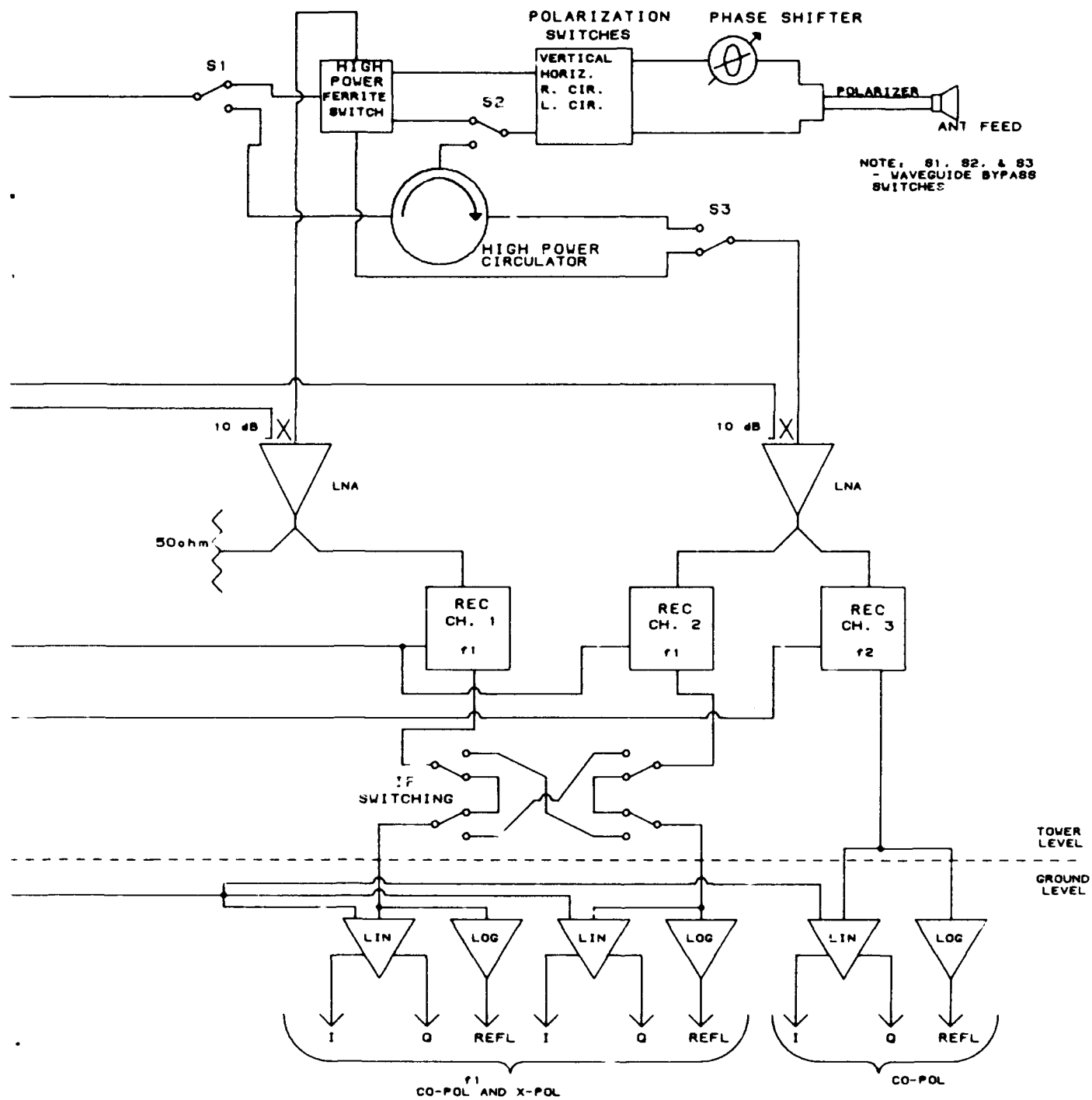


Figure 2. Engineering Diagram of the Radar System. Signal paths and specific components, such as master oscillator, klystrons, local oscillators, switches, and mixers, are identified. The antenna and radio-frequency polarization control components are on top of a 15-m tower; radio-



frequency receiver components, mixers, and intermediate-frequency switches and balancing components are in the tower, just below the antenna. Other components are in our instrumentation and analysis building near the base of the tower.

oscillators and the pulse generators are derived from a stabilized 5-MHz quartz oscillator, which exhibits extremely low phase noise and has a relative frequency stability of 3×10^{-12} during a millisecond. Each phase-locked oscillator drives a 2.5-W solid state amplifier, which provides the RF input to a high-power klystron. Each klystron (Varian Associates Model VA-87B) has a nominal peak output power of 1 MW. In each transmitter, the klystron is surrounded by an electromagnetic focus coil. Following the failure of several of the original water-cooled focus coils, we acquired and installed new air-cooled focus coils. The Experimental and Structural Support Branch of the laboratory constructed the housings and assembled the coils, using a design that had been developed at McGill University in Montréal and modified by the Design and Analysis Branch of the laboratory.

We usually run the transmitters at a peak output power between 470 and 680 kW and a pulse width of 1 μ sec. Each transmitter can be operated at pulse repetition times between 833 μ sec and 10 msec (pulse repetition frequencies between 100 and 1200 Hz). Because the average power capacity of the switchable circulators (described in Subsection 2.2) prevents concurrent operation of both transmitters at high power and high pulse repetition frequencies, we configured the system for full-matrix polarimetric measurements only with one transmitter operating. For this purpose we use a carrier frequency of 2.71 GHz and operate typically with a pulse repetition time of 1.03 msec (pulse repetition frequency 971 Hz), which yields an unambiguous range of 154.5 km and unambiguous Doppler velocity of $\pm 26.87 \text{ m sec}^{-1}$.

2.2. Polarization Control

Polarization of the transmitted and received signals is controlled in two stages by microwave devices mounted on one of the counterweight arms of the antenna. First, a network of three switchable ferrite circulators manufactured by Raytheon Co., Special Microwave Devices Operation, Northborough, Mass., alternates the polarization of successive pulses between two orthogonal states. Each of the three circulators is similar to those used in most radars that measure the linear polarization differential

reflectivity. The combination of three circulators yields a higher level of isolation between the transmission output ports and also provides reception ports for the backscattered signals. Operation of the switchable circulators is controlled by signals generated in the data processor, which also monitors the transmitted polarization. Parameters of the network of three circulators at the operating frequency of 2.71 GHz are listed in Table 1. For dual-frequency operation, which is limited to copolar reception, this network is bypassed by means of three solenoid-controlled mechanical switches, which are activated from the radar transmitter room.

The second stage of polarization control is a network of two solenoid-controlled mechanical switches and a 3-dB hybrid coupler manufactured by Atlantic Microwave Corp., Bolton, Mass., which allows the selection of either linear or circular polarization as the basis of measurements. For linear polarization, the waveguide switches direct the transmitted pulse into the coupler, where the power is divided equally between the two output ports and a 90° phase shift is introduced at one output port. The two signals pass through the waveguide switches again and are transmitted to the polarizer, where they combine to form either horizontal or vertical polarization. For circular polarization, the waveguide switches direct the transmitted pulses directly to the antenna, where they emerge as either right or left circularly polarized signals. Thus, in usual operation, the polarization of successive pulses is alternated either between horizontal and vertical or between right and left circular.

The signal at each receiver output port of the circulator network alternates between the copolarized and the cross-polarized components of the backscattered signal. A network of intermediate-frequency (IF) switches in the receiver lines (shown in Figure 2) compensates for the alternating polarization and assures that each set of receivers handles only the copolarized or the cross-polarized component. Control signals for these switches are generated in the data processor.

In June 1990 we identified a problem due to high-power RF energy coupling into the control circuitry for the switchable circulators. While this was being corrected we bypassed the switchable circulators temporarily, using the dual-frequency bypass (described above) for transmission and for reception of the copolarized signal through one set of receivers. We

connected the other port of the antenna directly to the other set of receivers for reception of the cross-polarized signal. The resulting half-matrix mode of operation permits us to pursue most of our scientific goals and is advantageous for evaluating the polarization characteristics of the antenna. Measurements in this mode can be compared with later measurements in the full-matrix mode to evaluate the performance of the antenna and the circulator network.

Table 1. Typical Parameters of Switchable Circulator Network. Values are referenced to output ports (to antenna) and associated receiver ports designated A and B with network set for transmission through Port A.

Parameter	Value
Transmission input port return loss	21.5 dB
Output port A return loss	26 dB
Output port B return loss	>40 dB
Receiver port A return loss	20 dB
Receiver port B return loss	23.5 dB
Isolation, input to output port B	≥ 40 dB
Insertion loss, input to output port A	1.5 dB
Insertion loss, output ports to receiver ports	<1 dB
Isolation, port A to port B	58 dB
Isolation, antenna to respective receiver port	65 dB

2.3. Antenna

From the polarization control components, two phase-balanced waveguides are connected to a sloped-septum polarizer and a scalar feed, which illuminates a paraboloidal reflector of 7.3-m (24-ft) diameter. The polarizer and feed are supported at the prime focus of the reflector by four struts, which are mounted orthogonally at 45° to the horizontal and vertical to reduce cross-polarization effects in side lobes. The level of illumination at

the edge of the reflector is -15 dB in both E and H planes. The on-axis gain of the antenna is 43.8 dB; the beamwidth of the main lobe, between the -3 -dB points, is 1.0° in azimuth and elevation; and the first side lobes are 29 dB or more below the peak of the main lobe.

The antenna and polarization control components are mounted on an elevation-over-azimuth pedestal capable of scanning continuously in azimuth and between 0° and 90° in elevation at a maximum rate of $15^\circ \text{ sec}^{-1}$. The antenna assembly is mounted on a 15.2-m (50-ft) tower (Air Force Type AB-563/GPS with 25-ft extension), so that the elevation axis is 20 m (65 ft) above ground level, or about 111 m (365 ft) above mean sea level. The antenna assembly is covered by a radome (Electronic Space Systems Corp. [ESSCO] Model M55-70-9000) of 17-m (55-ft) diameter. The radome, which was part of the original installation of the radar in 1980, is constructed of aluminum-framed triangular panels covered by ESSCOLAMTM laminated plastic membrane. The average area of a panel is about 2 m^2 , and the average length of a frame member is about 2 m. Because of the various shapes of the triangular panels, the frame of the radome is similar to a random-space-frame. Although it is obviously undesirable for polarimetric measurements, we are unable at the present time either to replace it or to perform the extensive weatherproofing that would be required for operation without a radome.

An antenna located on Nobscot Hill in Framingham, Mass., 8 km from our radar, provides us a limited capability for measurements of the radar antenna. The remote antenna, acquired from the Ipswich Electromagnetic Measurement Facility of the Rome Laboratory and refurbished by the Experimental and Structural Support Branch, can be rotated about its symmetry axis to generate a linearly polarized signal of arbitrary orientation. Use of this antenna for characterizing the polarimetric performance of the radar has proven difficult, however, because of multi-path propagation effects between the two antennas.

2.4. Antenna Control

The antenna may be controlled either manually or by means of a control program that runs on a Zenith personal computer. The antenna control program is modular and menu-based. At present it offers five functions, which are listed in the main menu shown in Figure 3a and described below. Selection of any one of these functions brings up a sub-menu, from which the parameters of the function are specified. In all the scanning functions, the most recently used values of the parameters are recovered as initial default values. If new values are entered, these become the default values for a subsequent entry to the function.

POINT AZ/EL: This function permits the user to direct the antenna to particular azimuth and elevation angles. The sub-menu (Figure 3a) displays the present azimuth and elevation angles of the antenna and allows the operator to specify either a new azimuth or a new elevation. When either is entered, the antenna drive responds and the new value is displayed. A pointing error of 0.05° is permitted.

PPI (Plan Position Indicator): This function yields continuous rotation in azimuth at a specified elevation angle. The sub-menu (Figure 3b) displays the specified elevation angle and the rate of rotation in azimuth. While the antenna is scanning, the display shows continuous readouts of the elevation angle, the azimuth angle, the azimuthal rotation rate, and a parameter related to the azimuth tachometer reading. The tachometer value is used to monitor the state of the antenna servo system; if it exceeds limits that are specified in the program, the antenna drive is shut down automatically to prevent damage.

VOLUME SCAN: This function generates a repeated sequence of azimuthal scans at specified elevation angles. Similar to the fundamental mode of operation of the WSR-88D (also known as the Next Generation Weather Radar [NEXRAD]), it is typically used to create an archive of data during a long period of time with minimally attended operation. The antenna scans continuously in azimuth; at each elevation angle the end of the scan overlaps the beginning slightly to assure continuity of the derived data arrays. The sub-menu (Figure 3c) permits the operator to specify the azimuthal rate of rotation and as many as nine elevation angles. Menu

```

##### ANTENNA CONTROL MENU #####
1.....POINT MODE
2.....AZIMUTH MODE
3.....ELEVATION MODE
4.....RETURN TO MAIN MENU
5.....EXIT PROGRAM

```

```

AZ = 221.00  EL = 1.40
POINT MODE
E.....ELEVATION
A.....AZIMUTH
R..RETURN TO MAIN MENU
ENTER SELECTION HERE > ENTER ELEVATION ANGLE >

```

Figure 3a. Menus of the Antenna Control Program, I. *Top*: Main menu identifies the five control functions. *Bottom*: *Point mode* directs the antenna to specified azimuth and elevation angles.

```

                                PPI MODE

1          Az SPD deg/sec      6.0
2          Elevation (deg)     .5

ENTER A "LINE #" TO MAKE A CHANGE ...
ENTER "S" TO START PPI SCAN .
ENTER "R" TO RETURN TO MASTER MENU ..

PLEASE ENTER YOUR SELECTION HERE >>
Chng El ang from .5 to

```

```

                                PPI MODE

1          Az SPD deg/sec      6.0
2          Elevation (deg)     .5

ENTER A "LINE #" TO MAKE A CHANGE ...
ENTER "S" TO START PPI SCAN .
ENTER "R" TO RETURN TO MASTER MENU ..

PLEASE ENTER YOUR SELECTION HERE >>
ENTER "R" TO RETURN TO MAIN MENU

ENTER "E" TO CHANGE PARAMETERS
El= .5 Az= 199.1 Az Spd= 5.8d/s  Lach= 78

```

Figure 3b. Menus of the Antenna Control Program, II. *Top: PPI mode* generates a continuous scan at a single elevation angle; initial entry "2" has generated the prompt to enter a new elevation angle. *Bottom: PPI mode* display shows antenna position and speed while the function is running.

```

                                VOLUME SCAN SUB MENU

                                EL STEP # 1 = .5
                                EL STEP # 2 = 1.0
                                EL STEP # 3 = 1.5
                                EL STEP # 4 = 2.0
                                # OF EL STEPS = 4
                                AZ SPD DEG/SEC = 6.0
                                VERT POINT OPTION IS OFF.

                                ENTER A "LINE #" TO MAKE A CHANGE ...
                                ENTER "S" TO START VOLUME SCANS ....
                                ENTER "R" TO RETURN TO MASTER MENU ..

                                PLEASE ENTER YOUR SELECTION HERE >>
                                Chng # of EL stps from 4 to

```

Figure 3c. Menus of the Antenna Control Program, III. *Volume scan* generates a series of slightly overlapping azimuthal scans at a succession of elevation angles; initial entry "A" has generated the prompt to enter a new number of elevation steps.

option "C" permits the antenna to be pointed toward the vertical for a specified length of time at the end of each volume scan. (This procedure was required for a particular measurement program several years ago and illustrates the way in which the antenna control program can be reconfigured to meet specialized objectives.) While the antenna is scanning, the display shows continuous readouts of the elevation and azimuth angles, the azimuth at which the next elevation step will occur, the antenna speed in degrees per second, and two parameters derived from the tachometer.

ELEVATION SECTOR: Also known as the Range Height Indicator (RHI) mode, this function generates one or more scans in elevation angle at specified azimuths. The sub-menu (Figure 3d) permits the operator to specify the angular limits and the scan speed and to select either single or multiple iterations of a procedure. Menu options 1 and 2 specify the starting and ending azimuth angles, and option 3 specifies the azimuthal increment. Whenever a new starting azimuth angle is specified, the ending azimuth angle is set equal to the starting angle; whenever the two azimuth angles are equal, option 3 is omitted from the display. If option 2 is used to specify a different ending azimuth angle, option 3 reappears in the display. Menu options 4 and 5 specify the limits of elevation angle. Menu option 6 is a toggle for single or multiple iteration of the procedure. Options 7 and 8 are related to the settings of horizontal and vertical scale factors on our displays. Option "A" specifies the maximum speed of the scan; this quantity is multiplied by the sine of the elevation angle to determine the actual speed of the antenna. This modification of the scan rate is used to assure adequate spatial sampling at low elevation angles and to slow the antenna gradually as it approaches its mechanical stops at 0° elevation angle. While the antenna is scanning, the display shows continuous readouts of the azimuth and elevation angles and two quantities that are used to monitor the antenna drive system.

AZIMUTH SECTOR: This function and its sub-menu (Figure 3e) are analogous to the Elevation Sector function described above. Menu options 1 and 2 specify the starting and ending elevation angles, and option 3 specifies the elevation increment. Whenever a new starting elevation angle is specified, the ending elevation angle is set equal to the starting angle; whenever the two elevation angles are equal, option 3 is omitted from the display. Menu options 4 and 5 specify the counterclockwise and clockwise

RHI MODE

```
1. START AZIMUTH FOR RHI = 50.0
2. END AZIMUTH FOR RHIs = 65.0
3. INCREMENTAL AZIMUTH = 5.0
4. LOWEST RHI ELEVATION = .5
5. HIGHEST RHI ELEVATION = 10.0
6. TOGGLE (S)ingle sequence/(C)ontinuous RHIs = S
7. ALT SCALE ON SCAN CONVERT = 8
8. RNG SCALE ON SCAN CONVERT = 4
9. ANT SPEED DEG/SEC = 4.0
```

TYPE "LINE 0" TO CHANGE PARAMETER
TYPE "S" TO START RHI SCANS
TYPE "R" TO RETURN TO MAIN MENU

PLEASE ENTER CHOICE HERE>>

Change High el from 10.0 to

Figure 3d. Menus of the Antenna Control Program, IV. *RHI mode* generates one or more elevation scans at specified azimuth angles; initial entry "5" has generated the prompt to enter a new upper limit of elevation angle.

SECTOR SCAN MODE

```
1...START ELEVATION FOR SECTOR SCAN = 1.2
2...END ELEVATION FOR SECTOR SCANS = 5.2
3...INCREMENTAL ELEVATION STEP = 1.2
4...START SECTOR AZIMUTH = 52.2
5...END SECTOR AZIMUTH = 82.2
6...TOGGLE (Single sequence/(Continuous) =
7...SECTOR SCAN SPEED DEG/SEC = 6.2
```

```
TYPE "LINE # " TO CHANGE PARAMETER
TYPE "S" TO START SECTOR SCANS
TYPE "F" TO RETURN TO MAIN MENU
```

ENTER CHOICE >>

Change Az start from 52.0 to

Figure 4c. Menus of the Antenna Control Program. A "sector scan mode" generates one or more azimuthal scans at specified elevation angles; initial entry "4" has generated the prompt to enter a new starting azimuth angle.

limits of azimuth angle, respectively. Menu option 6 is a toggle for single or multiple iteration of the procedure. Option 7 specifies the speed of the scan. While the antenna is scanning, the display shows continuous readouts of the azimuth and elevation angles and a parameter that is used to monitor the antenna drive system.

2.5. Receivers

The received signals are carried through coaxial cables (Cablewave Type HCC78-50J) from the antenna to the low-noise RF amplifiers, which are located in the tower about 7 m below the antenna. These amplifiers (Micromega Model 70149) are extremely stable; have level protection; exhibit a noise figure of 1.2 dB over the frequency band of 2.7–2.9 GHz; and have gain of 20 dB, input and output voltage standing wave ratio (VSWR) of 1.5:1, and maximum output power of +10 dBm for a 1-dB compression. For dual-frequency operation, when the switchable circulators are bypassed and the transmitted polarization is constant, a power divider and two band-pass filters separate the two carrier frequencies of the received signal (2.71 and 2.76 GHz) in the copolarized channel. Each RF filter reduces spurious signal levels from the other channel by more than 50 dB. In the cross-polarized channel there is a power divider and one band-pass filter (2.71 GHz). This configuration provides identical paths for the two signals of orthogonal polarizations. In each signal channel (two of 2.71 GHz and one of 2.76 GHz), a series of three circulators with carefully matched loads provides 90 dB of additional isolation. The combination of the power dividers, the bandpass filters, and the isolators provides more than 160 dB of isolation among the mixers at both RF and IF and prevents the generation of unwanted sidebands in the mixers. The signals are balanced in amplitude and phase before entering the mixers.

The mixers (RHG Model IRD2.7C14HB) are of the image-rejection quiet type and can accept input signals as high as 5 dBm. They are balanced to within $\pm 5^\circ$ in phase and within ± 0.5 dB in amplitude. The local oscillator frequencies for the mixers are derived from phase-locked oscillators that are driven by the 5-MHz master oscillator. The outputs of the phase-locked oscillators are bandpass filtered, isolated, amplitude balanced, and phase

balanced before being injected into the mixers at a power level of 13 dBm. The output of the mixers is the intermediate frequency of 30 MHz.

In single-frequency full-matrix polarimetric operations, each of the two receiver inputs alternates between the copolarized and cross-polarized signals, as noted in Subsection 2.2. The alternating polarizations are rectified by the IF switch network shown in Figure 2. Each signal is amplified by a low-noise IF amplifier and a high-performance amplifier to achieve the proper signal level for the linear and logarithmic amplifiers; the signals are level set, bandpass filtered, and amplitude balanced. The filters, manufactured by K & L Microwave, Inc., have a center frequency of 30 MHz, 3-dB bandwidth of 1.2 MHz, insertion loss of 4 dB, and VSWR of 1.5:1.

The signals are then carried about 25 m through coaxial cables to the IF receiver components, which are located in the instrumentation building in close proximity to the data processing and recording equipment. There they are received through phase quadrature receivers and logarithmic receivers to provide the complex amplitudes for Doppler signal processing and wide dynamic range for analysis of reflectivity and power ratios. In dual-frequency operation, the copolarized signal component from the 2.76-GHz carrier frequency is similarly processed, with the exception of the phase quadrature receiver. In the near future, we plan to replace the existing phase quadrature receivers and add one to the 2.76-GHz channel. The logarithmic receivers (RHG Model ICL30C14HA) have a minimum detectable signal of -112 dBm and a linearity of ± 0.5 dB over a dynamic range of 92 dB.

Receiver calibration is accomplished by using two phase-locked oscillators, which generate the two carrier frequencies of 2.71 and 2.76 GHz and are referenced to the 5-MHz master oscillator. These signals are injected into the respective receivers at predetermined power levels between 0 and -121 dBm through a Weinschel precision step attenuator. At each step the power level is held constant to within 0.1 dB by a comparison network that samples the output of the oscillator and controls a motorized attenuator. The calibration may be performed either manually or under computer control.

3. DATA ACQUISITION, DISPLAY, AND ANALYSIS

3.1. Real-time Processing, Archive, and Display

The complex amplitude and logarithmic power corresponding to the "main" backscatter channel (copolarized, if linear; cross-polarized, if circular) are processed in real time to yield averages of the reflectivity factor (Z) and the Doppler mean velocity in 1019 gates spaced 150 m apart between 0.6 and 153.3 km in range. These quantities are averaged and sampled at a selectable interval, typically 0.128 sec, which yields an azimuthal increment of 0.77° at an antenna speed of 1 revolution per minute. When the system is operated with linear polarization, the processor also yields the differential reflectivity, which is defined by

$$Z_{DR} = 10 \log (Z_H / Z_V), \quad (1)$$

where Z_H and Z_V denote the reflectivity factor measured with horizontal and vertical polarization, respectively.⁶ These quantities are displayed in real time, to guide the acquisition of polarimetric data, and also recorded for off-line analysis. Long-range surveillance is possible if the radar pulse repetition time is doubled and the processor is set to average rangewise pairs of data samples. The processor was designed and constructed by the Ground Based Remote Sensing Branch.^{7, 8}

3.2. Polarimetric Data Acquisition

In the full-matrix or half-matrix mode, the receiver output comprises the logarithmic power and the in-phase and quadrature components of the amplitude of each polarization. These six quantities are digitized and recorded as continuous time series in 50 selectable range gates for off-line analysis. Figure 4 shows a functional block diagram of the data acquisition system. A data acquisition control unit, also called the "time series electronics," was designed and constructed by the Ground Based Remote Sensing Branch. This unit allows a user to select the time delay to the first gate and the time increment between adjacent gates. The data are digitized

GEOPHYSICS DIRECTORATE

POLARIMETRIC TIMESERIES ACQUISITION SYSTEM

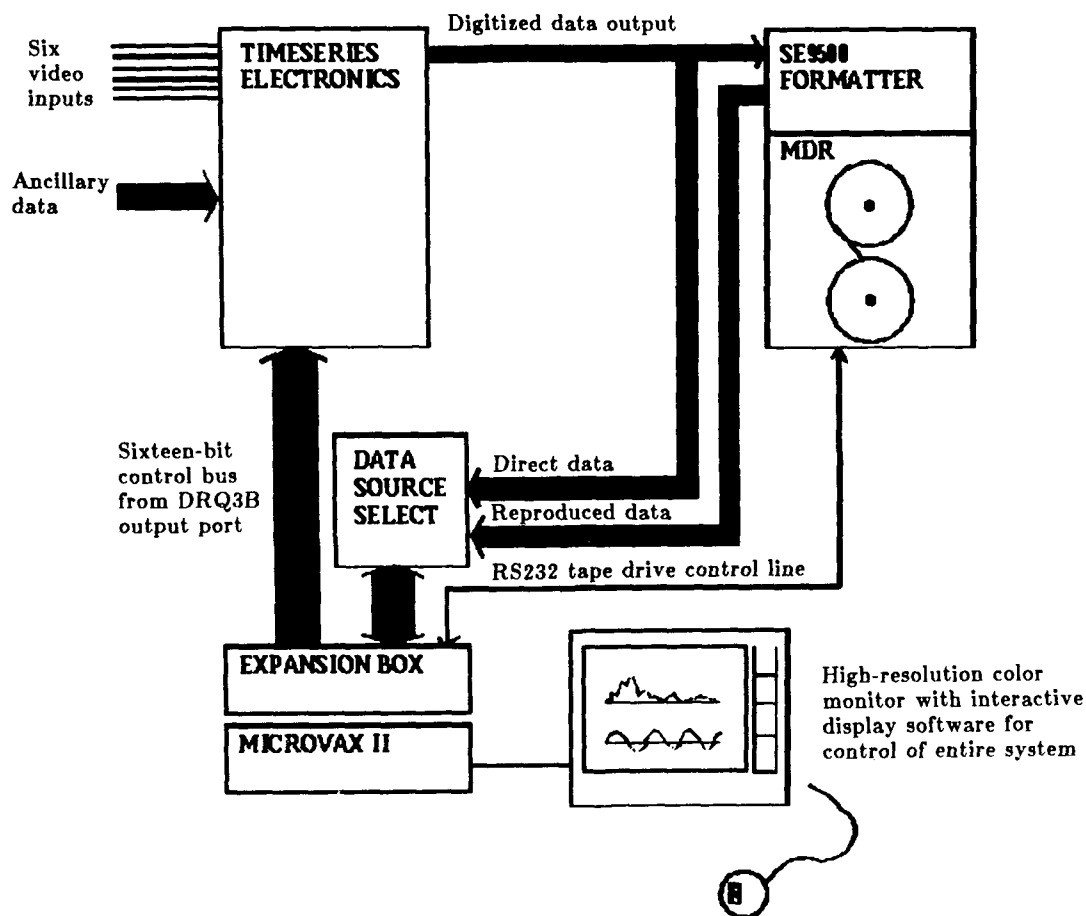


Figure 4. Functional Block Diagram of Data Acquisition System. Data acquisition unit, identified as "time series electronics," samples the six video inputs and the ancillary data for recording or display. Data acquisition control program on MicroVAX II workstation allows control of range gate settings and recorder operation. Program automatically selects reproduced data for real-time display whenever the data recorder is running.

(12 bits for logarithmic power and 8 bits for each of the in-phase and quadrature components), formatted in a Thorn EMI Datatech formatter, and recorded with a Penny and Giles high-density Multiband Data Recorder at a rate of approximately 500 kbyte sec⁻¹. Ancillary data include time, with millisecond resolution, and azimuth and elevation angles of the antenna. Time series up to one hour's duration are possible. Short segments of the time series (limited by the capacity of random access memory in the computer) can be captured in real time for quality assessment or analysis.

The data acquisition control unit and the data recorder can be controlled either manually or by means of a data acquisition control program that runs on a Digital Equipment Corp. VAXstation II/GPX workstation with a high-speed parallel interface controller and an RS-232 terminal controller. In the manual mode, the user selects the time delay to the first gate in microseconds and the time increment between adjacent gates as 1, 2, 4, 8, or 16 μ sec. The data control program permits the user to select the range to the first gate in kilometers and the range increment between gates as 150, 300, 600, 1200, or 2400 m by means of a mouse and an interactive display. Examples of the display are shown in Figures 5a and 5b. In addition to the main menu and sub-menus, the display includes samples of data from the six video inputs and information about present settings of radar and control parameters. Short segments of data, acquired at a selectable interval, are shown both as rangewise plots from the 50 gates and as time series from a selected gate. These data are acquired from the reproduce heads of the recorder if it is running; otherwise they are acquired directly from the data acquisition control unit. The positions of the 50 gates within the unambiguous range domain of the radar are also shown. The data control program allows full control of the data recorder, both for recording and for playback; the displays of data in range and time during playback are identical to those during recording.

The data acquisition procedure is as follows. First the operator turns on the radar and real-time displays and starts the antenna control program (described in Section 2.4). Next, the operator loads an archive tape on the multiband data recorder, turns on the data acquisition unit, and starts the data acquisition control program. For ease of operation, the personal computer on which the antenna control program runs is beside the

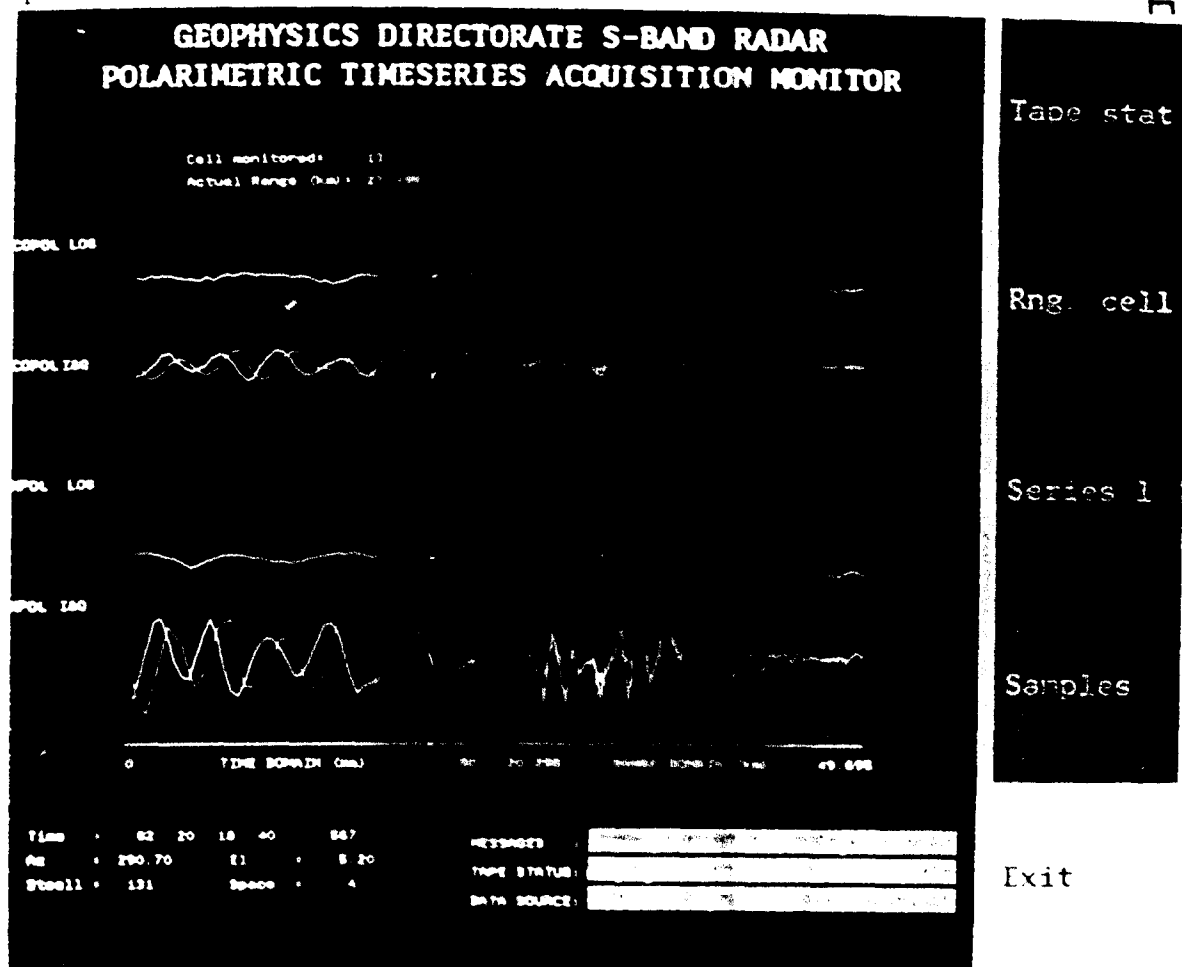


Figure 5a. Display of Data Acquisition Control Program, I. The top of the main window displays the logarithmic power and the in-phase and quadrature components of the copolarized received signal; the bottom of the main window displays the same quantities of the cross-polarized signal (the "main" component if circular polarization is transmitted). Rangewise profiles from the 50 gates are on the right; red circles mark the position of the gate from which time series are extracted for display on the left. Gate positions within the range domain of the radar are displayed in the small window immediately below. Window at lower left shows time of the displayed data (day, hour, minute, second, millisecond), antenna azimuth and elevation (degrees), and time delays to first gate and between gates (microseconds). Windows at lower right contain messages pertaining to system operation. Menu options in column at right are selected by means of a mouse.

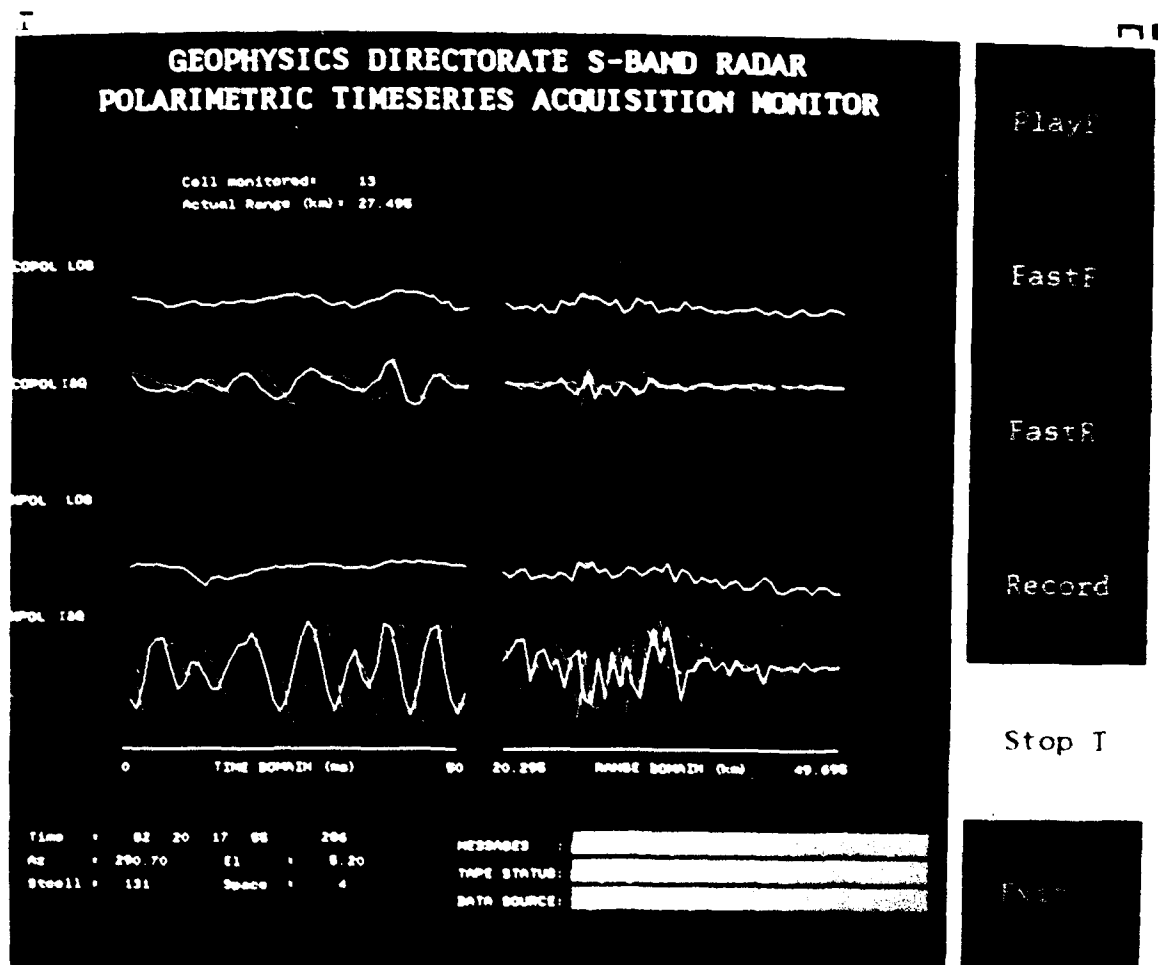


Figure 5b. Display of Data Acquisition Control Program, II. Selection of *Tape status* from menu shown in Figure 5a generates a submenu for control of the data recorder. Messages prompt user for input of a function command and show that the tape is playing forward at 30 inches per second.

workstation on which the data control program runs. An oscilloscope alongside provides an "A-scope" display of either of the logarithmic power signals and also displays the positions of the 50 gates. The data acquisition unit, multiband data recorder, and real-time displays are nearby. Thus, when a region of interest is identified on the real-time displays, the operator can turn the antenna to appropriate coordinates, set the positions of the 50 gates, initiate a scanning procedure, and start the recorder. For later reference, the antenna control program writes a disk file of all antenna movements and the data control program writes a disk file of all commands sent to the data acquisition unit and the recorder.

3.3. Analysis

Data analysis is supported by a cluster of computers manufactured by Digital Equipment Corp. (DEC), including a MicroVAX 3100/20 computer and five MicroVAX II/GPX microcomputers, three of which have high-speed parallel interface controllers for real-time data acquisition. These computers also support other programs at the field site in Sudbury. Output devices include a DEC LJ250 color printer and a Seiko CH-5301 Hardcopier, each of which produces images in full color on either paper or transparency stock. Data storage media include standard 1600 and 6250 BPI tapes and DEC TK-50 tape. The local cluster is connected to computers at Hanscom Air Force Base through a dedicated 9600-baud line that gives us access to additional capability, including archived weather data and worldwide computer networks.

Transfer of the polarimetric data into a computer is limited, as noted above, by the capacity of random access memory. Long time series can be generated on disk or tape by the merging of successive segments read from the archive tape. By means of a data merging program, the user specifies the starting time and length of series; the program advances or rewinds the archive tape to the starting time and determines the requisite number of segments to be read. A slight overlap of the successive segments assures continuity in the synthesized time series. With our present computer capability, the time required to synthesize a long series of data is about 60 times the length of the series.

4. MEASUREMENTS

There are three main objectives for our initial measurements and analyses: (1) to characterize the polarimetric performance of the radar, (2) to describe microphysical attributes of cloud and precipitation particles, and (3) to identify the effects of changing electric fields on the orientations of hydrometeors,⁴ which is our primary scientific emphasis at present. Most of our full-matrix and half-matrix measurements and all of the measurements described below have been made with circular polarization, so that the "main" component of the backscatter from hydrometeors is received in the channel orthogonal to the channel of transmission. Our approach to data analysis emphasizes the computation and interpretation of power ratios, cross-correlations, Doppler spectra and cross-spectra, and Doppler mean velocities of differently polarized signals.⁹

From several observations of light and moderate rain at vertical incidence we have made preliminary estimates of the polarimetric error parameters of the radar. We use the techniques developed by McCormick and Hendry,¹⁰ who defined the relative amplitude ϵ of polarization error in the radiated signal, that is, the departure from the nominal polarization state. Because small raindrops appear nearly circular when viewed at vertical incidence, radar observations under these conditions provide estimates of the mean error amplitude and phase, the mean squared error amplitude, and the variance of the error amplitude, all of which are power-weighted averages across the radar beam. Specifically, we examine the circular depolarization ratio,

$$\text{CDR} = 4 \overline{\epsilon^2}, \quad (2)$$

the cross-correlation,

$$\rho = \overline{\epsilon} / (\overline{\epsilon^2})^{1/2}, \quad (3)$$

and the cross-covariance amplitude ratio,

$$\text{CCAR} = \rho \times (\text{CDR})^{1/2} = 2 \overline{\epsilon}, \quad (4)$$

where ϵ is assumed to be much less than unity. One of these observations, made on 15 April 1991, is shown in Figure 6. The antenna was rotated through one full revolution during the one-minute observation, to reveal any azimuth dependence of the observed effects. The first gate was set at 645 m, and the increment between the gates was 150 m. Hydrometeor backscatter was detected to a height of about 6.5 km, with a melting layer evident in the high values of the circular depolarization ratio near 3.6 km. The lowest observed value of the CDR in the rain, indicative of the error limit of the radar, is -26.3 dB, which implies a mean squared error amplitude of 5.86×10^{-4} . In the region where the CDR is low, the cross-correlation between the right and left circularly polarized signals is about 0.1 (10%). From these quantities we deduce that the magnitude of the CCAR is 4.84×10^{-3} and the mean error amplitude is 2.42×10^{-3} . Because the mean error amplitude is so small, the mean squared error amplitude is nearly equal to the variance of ϵ , and the lowest observed CDR essentially defines the measurement limit of the radar. The phase of the cross-covariance of the orthogonally polarized signals passes through two full cycles as the antenna rotates once. This characteristic may be due to an azimuth-dependent phase shift in the azimuth rotary joint of the antenna mount; further measurements of the radar and its components will be necessary to characterize this effect.

An example of our investigation of hydrometeor microphysics is the observation of melting stratiform precipitation made on 21 April 1991 and shown in Figures 7a and 7b. This observation is a vertical cross-section derived from an elevation scan from 0.5 to 60° . The reflectivity shows a distinct "bright band," associated with initiation of the melting process, at about 3 km height. Beyond about 15 km distance, the bright band is weaker, due probably to a lower precipitation rate in that region and to the greater width of the radar beam at greater range. The CDR exhibits maximum values above -8 dB just below the height of the reflectivity bright band at ranges less than about 15 km. These values are probably due to the presence of highly non-spherical, nearly melted hydrometeors. At greater ranges the maximum of the CDR nearly coincides with the reflectivity maximum, indicating different characteristics of the hydrometeors there. The cross-correlation of the right and left circularly polarized signals is primarily indicative of the degree of common orientation

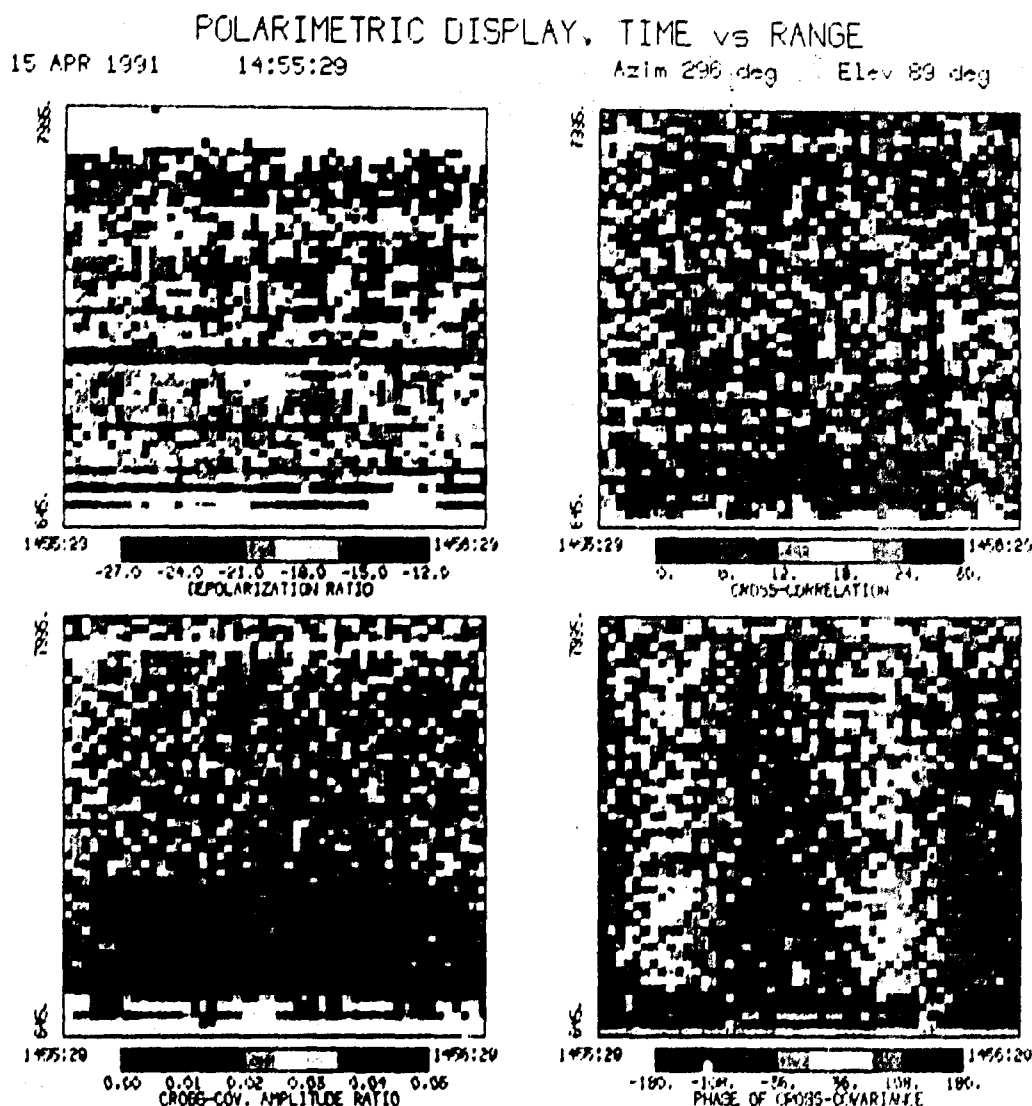


Figure 6. Radar Measurements of Light Rain at Vertical Incidence. The antenna was rotated through 360° during a one-minute observation on 15 April 1991, beginning at 14:54:30 EST, while the rainfall rate was 2.9 mm hr^{-1} . Because small raindrops appear circular when viewed from below, measurements at vertical incidence in light rain reveal polarimetric attributes of the radar system. *Upper left:* Circular depolarization ratio (decibels) provides an estimate of the mean squared error amplitude. *Upper right:* Cross-correlation of the right and left circularly polarized signals (per cent) is related to the variance of the error amplitude. *Lower left:* Cross-covariance amplitude ratio (dimensionless) provides an estimate of the mean error amplitude. *Lower right:* Phase of the cross-covariance of the orthogonally polarized signals (degrees) provides an estimate of the electromagnetic phase of the error.

POLARIMETRIC DISPLAY, ELEVATION SECTOR

21 APR 1991

12:12:49

Azlm 144 deg

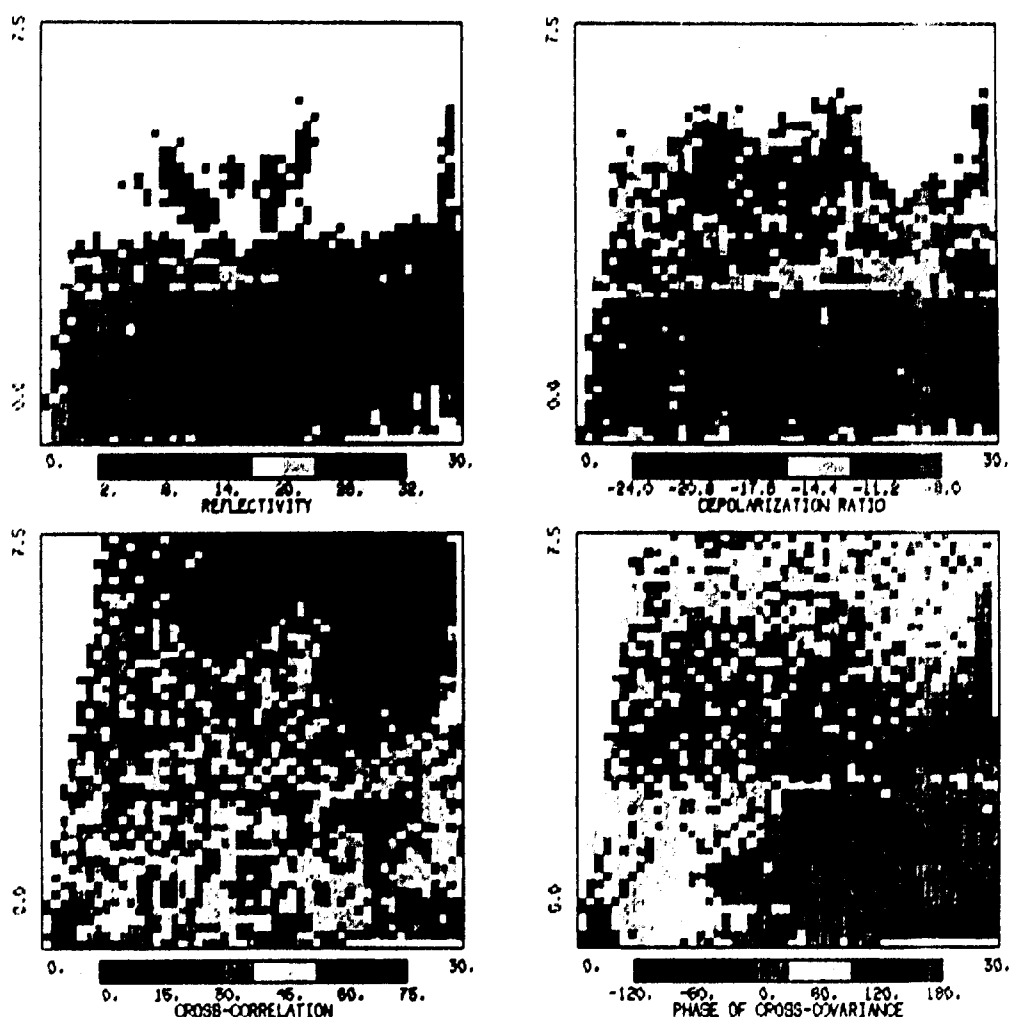


Figure 7a. Radar Observation of Melting Precipitation, 1. Elevation scan from 0.5 to 60° through stratiform precipitation was made on 21 April 1991. Display domain is from 0 to 30 km horizontally and 0 to 7.5 km above ground level. Displayed quantities include (upper left) reflectivity (dBZ), (upper right) circular depolarization ratio (decibels), (lower left) cross-correlation of the right and left circularly polarized signals (per cent), and (lower right) phase of the cross-covariance of the right and left circularly polarized received signals (degrees). Details are discussed in the text.

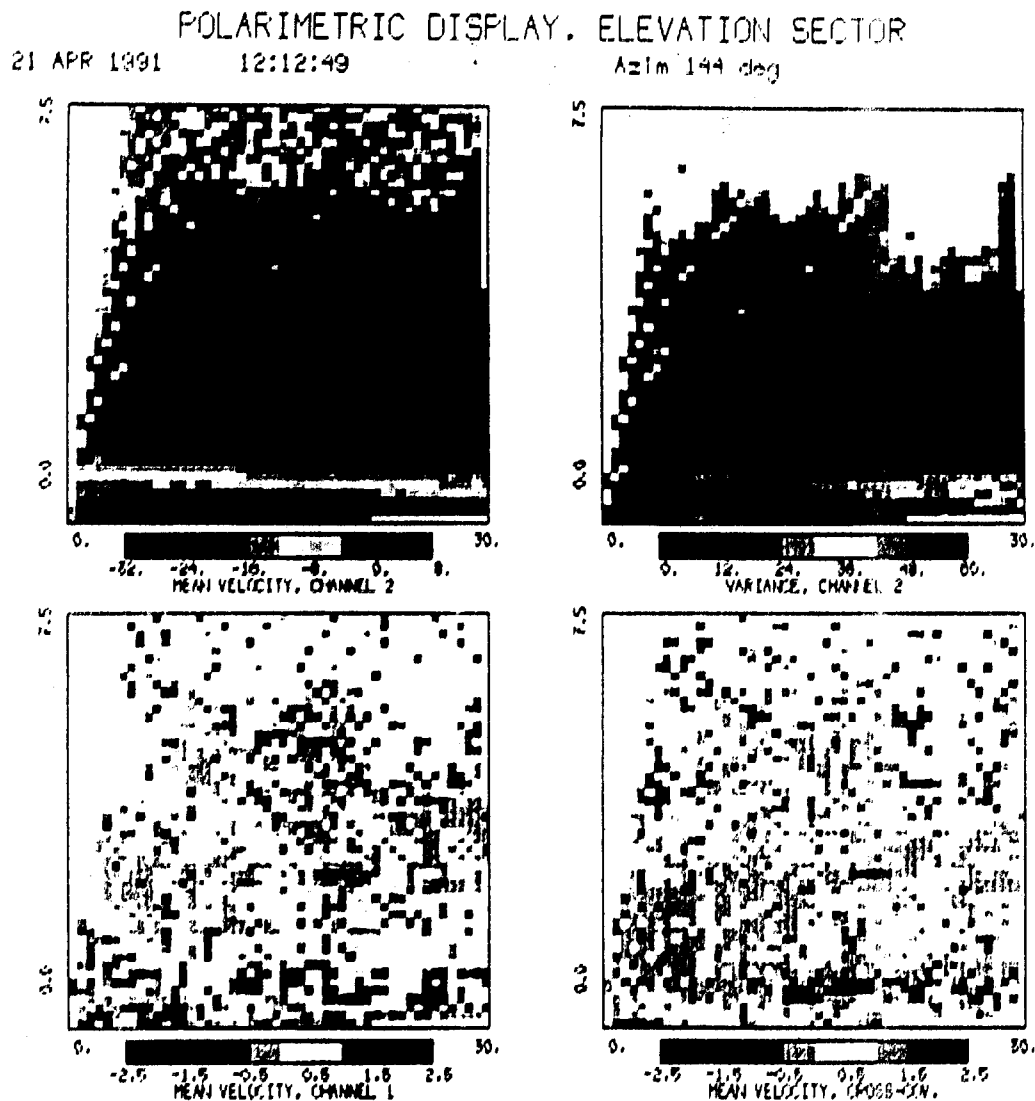


Figure 7b. Radar Observation of Melting Precipitation, II. Displayed quantities include (*upper right*) Doppler mean velocity (m sec^{-1}) derived from the main channel of backscatter, (*upper right*) Doppler spectrum variance ($\text{m}^2 \text{sec}^{-2}$) derived from the main channel, (*lower left*) difference of Doppler velocities derived from the transmission channel and from the main channel (m sec^{-1}), and (*lower left*) difference of Doppler velocities derived from the cross-covariance and from the main channel (m sec^{-1}). Details are discussed in the text.

of the hydrometeors. High values, ranging from 50 to 70%, occur below the melting level. The absence of values above 90%, which are expected in rain, is probably due to the weak signal received in the transmission channel. The phase of the cross-covariance of the orthogonally polarized signals contains information about hydrometeor canting and differential propagation effects. The increase of the phase angle with range, from near 150° to near 0° in the first 15 km at low altitude, reveals a propagation effect in the heaviest rain. The Doppler mean velocity derived from the main channel of backscatter (orthogonal to the transmission channel, for circular polarization) shows a layer of strong shear at about 1 km height between a weak outward flow near the surface and strong inward flow aloft. The Doppler spectrum variance is largest in the strongly sheared layer; elsewhere it is less than $10 \text{ m}^2 \text{ sec}^{-2}$, except at higher elevation angles in the rain, where the distribution of fall speeds is a significant component. The difference of the Doppler velocities derived from the transmission channel and the orthogonal ("main") channel shows the motion of the most non-spherical hydrometeors relative to the motion of all the hydrometeors. The observed characteristics differ from theoretical predictions, which state that in the present situation this quantity should be slightly negative in the lowest 3 km due to the sheared flow there. The observed characteristics may be due in part to the low power of the signal received in the transmission channel, which is close to the minimum detectable level in much of the region beyond 15 km range at low altitude. The difference of the Doppler velocities derived from the cross-covariance and from the "main" channel shows the motion of the hydrometeors having the highest degree of common orientation relative to the motion of all the hydrometeors. Negative values observed in the lowest 3 km, particularly in the layer of strongest shear, are qualitatively consistent with theoretical predictions.

In our investigation of electrical effects on hydrometeor orientations, we are attempting initially to determine the detectability of the phenomena that have been observed with radars of 1.8 cm^{11, 12} and 3.1 cm wavelength.¹³ Typically, we point the radar beam into an electrically active region for several minutes, observe the received signal on the "A-scope," and note the times of lightning discharges that intersect the beam. We later examine short segments of data centered near these times. Our

early results show that the change of CDR associated with a rapidly changing electric field is typically only 1–2 dB. The magnitude and phase of the cross-correlation provide more reliable indicators of the changing electric field, although the changes of these quantities are also small. Changes of 15–20% and 20–40° appear typical. Most of the events we have observed span only a few kilometers in range. One observation on 17 May 1991, shown in Figure 8, indicates a change of electric field spanning an exceptionally large range domain. In this example the lightning is evident in the reflectivity and the CDR in pixels 28–30 in time (about 1900:53 EST). It is more readily seen in the CDR (range gates 17–26) than in the reflectivity because the backscatter from the lightning plasma is less masked by hydrometeor backscatter in the transmission channel than in the "main" channel. In range gates 20–42 for several seconds before the lightning the cross-correlation is between 6 and 48% and the phase is between –90 and +60°; for several seconds after the lightning, the cross-correlation is between 18 and 60% and the phase is between –80 and 0°. Individual range gates show changes of 12–18% (2–3 quantization levels in the image) in cross-correlation and about 40° (2 quantization levels) in phase.

We expect to continue these observations through the summer and fall of 1991 to refine our experimental procedures and increase our data base. Our next step will be to investigate the spatial structure and variability of the orientation effects, by means of repeated scans of small sectors. We have attempted a few observations of this type but have not yet fully analyzed them.

5. RELATED FACILITIES

The Geophysics Directorate operates other equipment at the field site in Sudbury, Mass., in addition to the 11-cm polarimetric Doppler radar. Of particular importance to research relating to cloud and precipitation microphysics are two RD-69 raindrop distrometers, manufactured by Distromet, Ltd., Basel, Switzerland; tipping-bucket raingauges with expanded collection funnels; and a vertically pointing 8.6-mm wavelength TPQ-11 radar. Reflectivity data from the TPQ-11 radar can be sampled in

POLARIMETRIC DISPLAY, TIME vs RANGE

17 MAY 1991 19: 01:42 Azim 94 deg Elev 9 deg

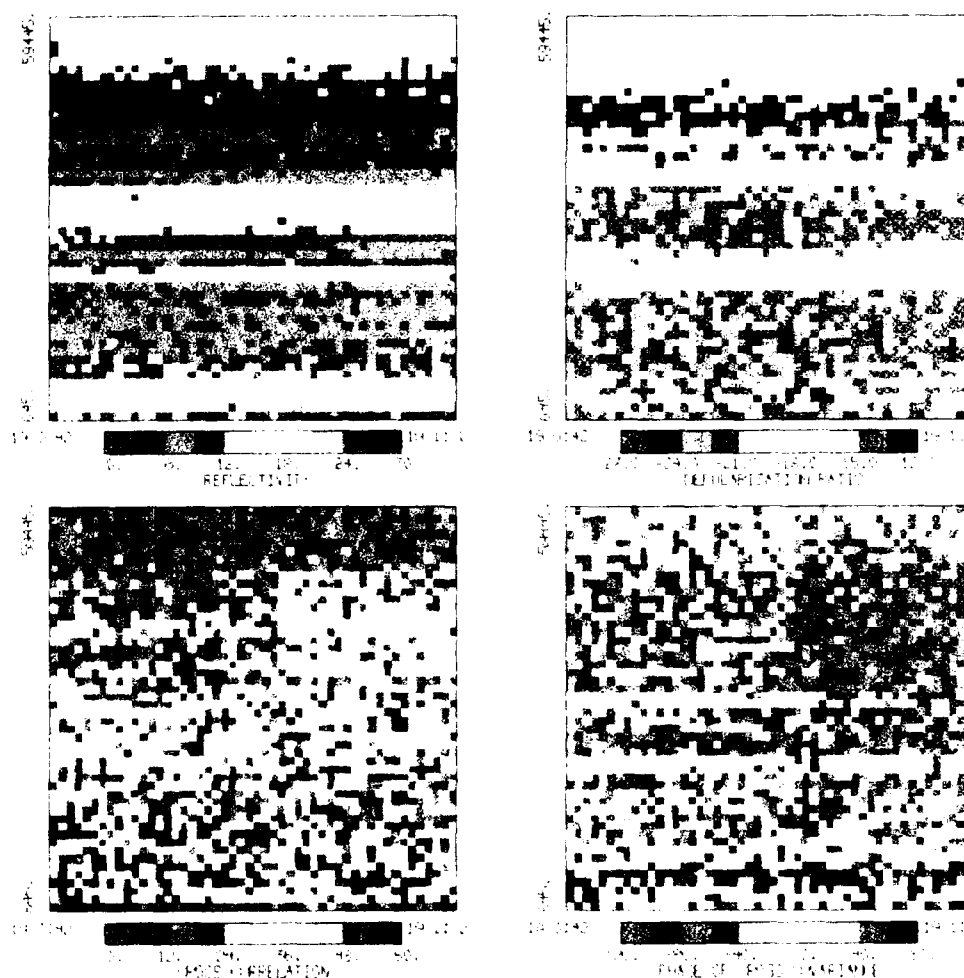


Figure 8. Radar Observation of Lightning and Changing Electric Fields. Thunderstorm was observed on 17 May 1991. Antenna was held stationary at 94° azimuth and 9° elevation. Range domain 0.6–59.4 km corresponds to heights of 0.1–9.3 km. Time domain of display is 20 sec. *Upper left:* Reflectivity (dBZ) shows momentary increase due to backscatter from the ionized lightning channel superimposed on the nearly constant hydrometeor backscatter. Duration of lightning channel is about 0.8 sec (two pixels). *Upper right:* Circular depolarization ratio (decibels) exhibits values near zero decibels (exceeding the present color scale) due to the backscatter from lightning, but no discernible change in the hydrometeor backscatter at the time of the lightning. *Lower left:* Cross-correlation of orthogonally polarized signals (per cent) exhibits a marked increase at all ranges between 23 and 50 km (cells 20 and 42) coincident with the lightning. *Lower right:* Phase of the cross-covariance of orthogonally polarized signals (degrees) exhibits a slight change coincident with the lightning.

POLARIMETRIC DISPLAY, TIME vs RANGE

17 MAY 1991 19: 0:42 Azim 94 deg Elev 9 deg

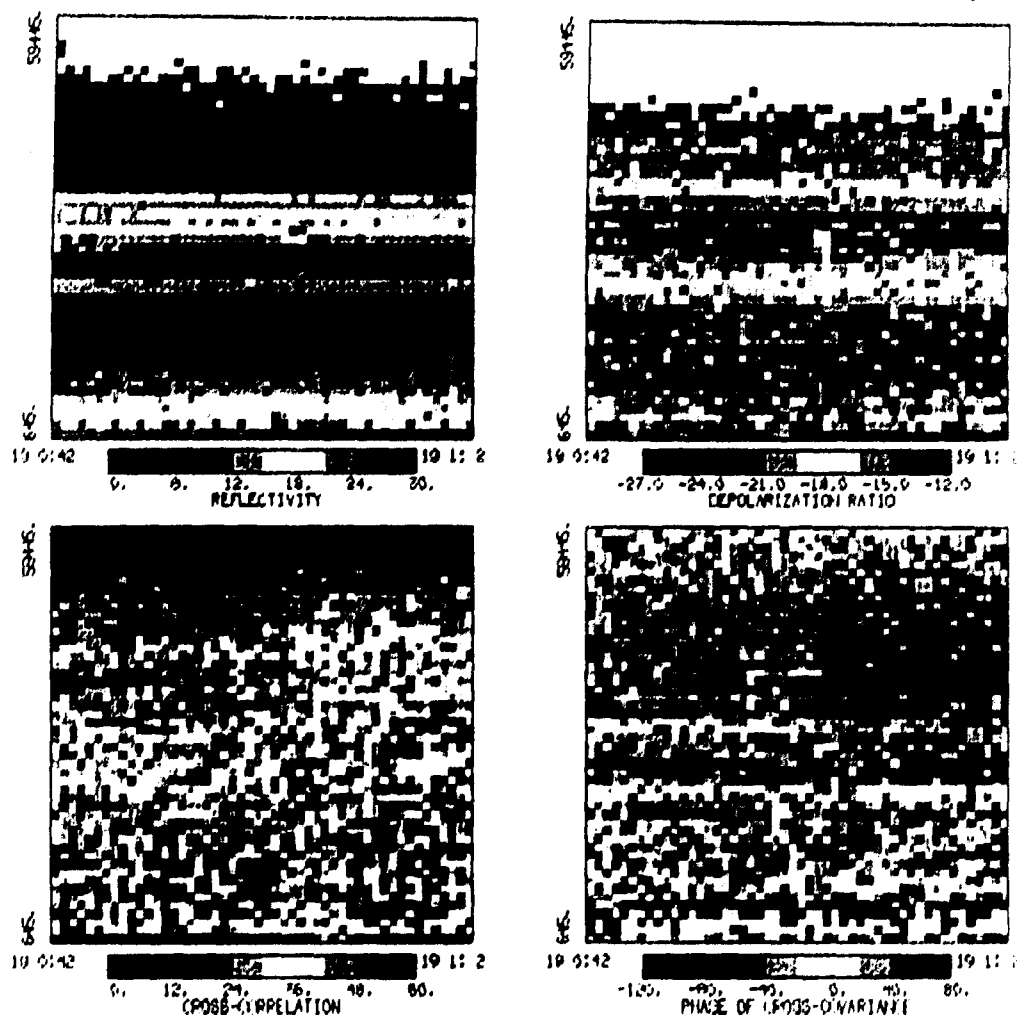


Figure 8. Radar Observation of Lightning and Changing Electric Fields. Thunderstorm was observed on 17 May 1991. Antenna was held stationary at 94° azimuth and 9° elevation. Range domain 0.6–59.4 km corresponds to heights of 0.1–0.3 km. Time domain of display is 20 sec. *Upper left:* Reflectivity (dBZ) shows momentary increase due to backscatter from the ionized lightning channel superimposed on the nearly constant hydrometeor backscatter. Duration of lightning channel is about 0.8 sec (two pixels). *Upper right:* Circular depolarization ratio (decibels) exhibits values near zero decibels (exceeding the present color scale) due to the backscatter from lightning, but no discernible change in the hydrometeor backscatter at the time of the lightning. *Lower left:* Cross-correlation of orthogonally polarized signals (per cent) exhibits a marked increase at all ranges between 23 and 50 km (cells 20 and 42) coincident with the lightning. *Lower right:* Phase of the cross-covariance of orthogonally polarized signals (degrees) exhibits a slight change coincident with the lightning.

248 range gates spaced 75 m apart, averaged in time increments of 1 sec (1024 pulses), displayed on a high-resolution color monitor, and recorded digitally for subsequent analysis. Investigations of cloud electrification and lightning will be aided by an electric field change sensor, also known as a "slow antenna." This antenna is being constructed by the Ground Based Remote Sensing Branch, with support from the Experimental and Structural Support Branch, during the summer of 1991. A 404-MHz Doppler radar, manufactured by Unisys Corp., is in continuous operation as a wind profiler. We plan to add an acoustic transmission capability within the next year to create a radar-acoustic sounding system (RASS), capable of measuring vertical profiles of both wind and temperature. A mobile LORAN radiosonde system is available for *in situ* wind and temperature sounding.

At Hanscom Air Force Base the Atmospheric Sciences Division of the laboratory receives and archives surface and upper air observations and a variety of meteorological imagery obtained from satellites. These data are used to support several scientific programs in other branches of the Division. The Division also receives and archives lightning location data from the network operated by the State University of New York at Albany.

The Massachusetts Institute of Technology (MIT) operates an 11-cm Doppler radar in Cambridge, Mass., 33 km from our radar. On several occasions this radar has been used in coordination with ours to observe lightning or to acquire Doppler velocity data for synthesis of two-dimensional wind fields. Individuals who anticipate a need for data from this radar should contact the Department of Earth, Atmospheric, and Planetary Sciences at MIT, as we have no formal agreement with MIT for exchange of radar data.

6. SUMMARY

The Geophysics Directorate operates a unique full-matrix coherent 11-cm (S-band) meteorological radar. It was developed to serve a variety of purposes in cloud physics research and analytical technique development. Pulse-to-pulse switching of the transmitted polarization permits

measurement of the full polarimetric backscatter matrix. Either circular or linear polarizatic may be used. The polarimetric data are recorded as time series for off-line analysis. Thus, the system not only yields measurements of differential reflectivity, differential phase shift, and terms of the covariance matrix but also can support investigations of advanced polarimetric data processing concepts. Operation of the radar for meteorological measurements mainly involves control of the antenna and control of the data acquisition, which are described in detail in Subsections 2.4 and 3.2, respectively. We welcome inquiries from individuals who are interested in collaborative experiments.

References

1. Bishop, A. W., and Armstrong, G. M. (1982) *A 10 cm Dual Frequency Doppler Weather Radar, Part I: The Radar System*, AFGL-TR-82-0321(I), AD A125885.
2. Metcalf, J. I. (1988) *Precipitation and Lightning Measurements by Polarization Diversity Radar*, AFGL-TR-88-0215, AD A213810.
3. Metcalf, J. I., and Ruggiero, F. H. (1990) *Mesoscale Features of a Winter Storm: Dual-Doppler Velocity Fields and Differential Reflectivity*, GL-TR-90-0091, AD A227342.
4. Metcalf, J. I. (1989) *Radar detection of lightning and electric fields*, GL-TR-89-0223, AD A217894.
5. Bishop, A. W., and Metcalf, J. I. (1985) *A Multi-Channel Radar Receiver*, AFGL-TR-85-0006, AD A156058.
6. Seliga, T. A., and Bringi, V. N. (1976) Potential use of radar differential reflectivity measurements at orthogonal polarizations for measuring precipitation, *J. Appl. Meteorol.*, **15**:69-76.
7. Metcalf, J. I., and Armstrong, G. M. (1983) *A Polarization Diversity Radar Data Processor*, AFGL-TR-83-0111, AD A134011.

8. Metcalf, J. I., Armstrong, G. M., and Bishop, A. W. (1987) *A Polarization Diversity Meteorological Radar System*, AFGL-TR-87-0105, AD A189291.
9. Metcalf, J. I. (1986) Interpretation of the autocovariances and cross-covariance from a polarization diversity radar, *J. Atmos. Sci.*, **43**:2479–2498.
10. McCormick, G. C., and Hendry, A. (1979) Techniques for the determination of the polarization properties of precipitation, *Radio Sci.*, **14**:1027–1040.
11. Hendry, A., and McCormick, G. C. (1976) Radar observations of the alignment of precipitation particles by electrostatic fields in thunderstorms, *J. Geophys. Res.*, **81**:5353–5357.
12. Hendry, A., and Antar, Y. M. M. (1982) Radar observations of polarization characteristics and lightning-induced realignment of atmospheric ice crystals, *Radio Sci.*, **17**:1243–1250.
13. Krehbiel, P., McCrary, S., Rison, W., Blackman, T., and Brook, M. (1989) Initial radar observations of lightning echoes and precipitation alignment at 3 cm wavelength, Fall Meeting (San Francisco), Amer. Geophys. Union; *Eos, Trans. Amer. Geophys. Union*, **43**:1028 (abstract only).